BEAM TRANSFORM METHOD FOR PLANE WAVE RESPONSE MATRICES

R. J. Adams

Dept. of Electrical Engineering, University of Kentucky
Lexington, KY 40506-0046, USA

F. X. Canning

Simply Sparse Technologies, Inc.
Morgantown, WV, USA

F. Mev

University of Kentucky
Lexington, KY, USA

B. A. Davis

NanoSonic, Inc.
Blacksburg, VA, USA

Abstract—A single-level compression algorithm is described for the plane wave response matrix, which defines the current excited on the surface of a scatterer by a spectrum of incident plane waves. The reported method is based on the physical principle that it is often possible to organize plane waves originating from a given angular region to form incident beams which excite localized currents on the surface of an electrically large target. The properties of the method are illustrated for several scattering problems in two dimensions.

1 **Introduction**

2 **A Model Problem**

3 **The P-Matrix**

1. INTRODUCTION

Numerical solutions of surface integral equation formulations of time-harmonic electromagnetic radiation and scattering from perfectly conducting targets involve solving linear systems of the form [1]

$$M^i = ZJ, \tag{1}$$

where Z is the impedance matrix, the vector J contains the coefficients of the basis functions used to represent the electric currents on the surface of an obstacle, and the vector M^i is determined by impressed sources.

The use of surface integral equations usually leads to a full impedance matrix. As a result, the computational costs associated with standard solutions of (1) are prohibitive for electrically large problems, and it is often necessary to solve (1) iteratively using compression algorithms for the impedance matrix [2]. However, the computational costs of fast iterative solvers can be significant when the impedance matrix is poorly conditioned, and when solutions are required for a large number of excitations.

A general scheme for addressing the limitations associated with fast iterative solvers for electrically large problems should have two properties. First, it should provide a computationally efficient representation for the inverse of the impedance matrix, Z^{-1}. To be generally applicable, such a scheme should also provide an efficient

procedure to determine the compressed representation of the inverse from more directly available information, such as that contained in (1).

In this paper we restrict our attention to the first of these requirements. Furthermore, instead of working directly with the inverse of the impedance matrix, we present a compression algorithm for a related problem. The algorithm we report compresses the plane wave response matrix (P-matrix) which specifies the currents excited on the surface of a target by a spectrum of incident plane waves.

The motivation for working with spectrally forced representations of the scattering problem instead of working directly with the spatial domain representation indicated by (1) follows from the physical characteristics of wave phenomena. For many electrically large scattering problems, with proper weighting, it is possible to group plane wave sources originating from a small spread of angular directions in order to form incident beams which excite surface currents that are nonzero over a small fraction of a large obstacle. Using this principle, we demonstrate that it is possible to determine a sequence of linear transformations in the domain of the P-matrix which yield sparse representations for electrically large problems.

The remainder of this paper is organized as follows. A class of two-dimensional scattering problems is defined in Section 2. These problems are used in the remainder of the document to illustrate the properties of the BTM. The plane wave response matrix is defined in Section 3, and its relationship to the impedance matrix of (1) is identified. The spatial and angular groupings used by the BTM are defined in Section 4. The single-level BTM is summarized in Section 5, and numerical results obtained by applying the BTM to the problems defined in Section 2 are reported in Section 6. A summary and discussion of the BTM are provided in Section 7.

2. A MODEL PROBLEM

The beam transform method is illustrated below for the two-dimensional problem of TM_z scattering from open, perfectly conducting cylinders. In this case the integral equation for the normal derivative of the electric field satisfies [1]

$$0 = E_z^i(\boldsymbol{\rho}) - \int\limits_C G(\boldsymbol{\rho}, \boldsymbol{\rho}) \frac{\partial E_z(\boldsymbol{\rho}')}{\partial n} dC', \qquad (2)$$

where G is the two-dimensional Green function, and C denotes the contour which defines the target. Finite projections of (2) will be obtained using a point-matching moment method discretization [1].
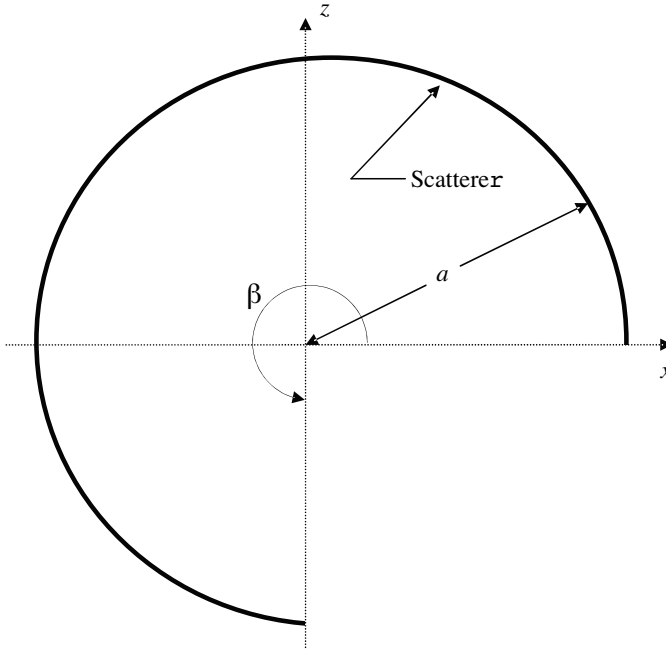
Figure 1. Properties of the BCM are illustrated for TM_z scattering from open, perfectly conducting cylinders with radius a and interior angle β. When $\beta = 2\pi$, the open problem reduces to the problem of scattering from a closed circular cylinder.

This reduces (2) to a matrix equation with the form indicated in (1) where M^i consists of samples of the incident field E_z^i, and J contains the coefficients of the pulse basis functions used to expand the normal derivative of the z-directed electric field.

In the remainder of this document we will restrict our consideration to the linear systems obtained when a discrete form of (2) is used to model scattering from the set of targets indicated by Figure 1. Although relatively simple, these systems have several features which make them numerically interesting. First, discrete forms of (2) are poorly conditioned. For all $\beta < 2\pi$, the geometries illustrated in Figure 1 are open. For TM_z polarization, this implies that the solutions to (2) are singular in neighborhood of $\phi = 0$ and $\phi = \beta$. Finally, when β is near 2π, the geometry of Figure 1 is quasi-resonant, implying that (2) incorporates strong, physical multiple scattering interactions. These features make iterative solution methods for this class of problems computationally expensive.

3. THE P-MATRIX

Instead of directly considering compression methods for the inverse impedance matrix, we consider the related problem of compressing the plane wave response matrix (P-matrix), which defines the currents excited on the surface of a target by a spectrum of incident plane waves. While the P-matrix itself provides adequate information for a number of important applications, we expect that it might also be useful in developing more general representations for Z^{-1}.

The P-matrix is obtained by assuming that the incident electric field can be expanded as a sum of propagating plane waves:

$$E_z^i(\boldsymbol{\rho}) = \frac{1}{2\pi} \int\limits_{2\pi} e^{j\mathbf{k}\cdot\boldsymbol{\rho}} f^i(\phi) d\phi, \tag{3}$$

where $\mathbf{k} = k(\hat{\mathbf{x}}\cos\phi + \hat{\mathbf{y}}\sin\phi)$, $k = 2\pi/\lambda$ and $f^i(\phi)$ is the plane wave spectrum of the incident field. In the following we denote the discrete form of (3) as

$$E_z^i = D f^i, \tag{4}$$

where D is a discrete representation of the continuous integral operator appearing in (3). In the numerical examples considered below, the vectors E_z^i and f^i are obtained as point samples of their continuous counterparts. Similarly, the elements of D are point samples of $e^{j\mathbf{k}\cdot\boldsymbol{\rho}}$ multiplied by $1/N_\phi$, where N_ϕ is the number of uniformly spaced samples used to discretize (3).

For the class of problems indicated by (2) and (3), Equation (1) becomes

$$ZJ = M^i = D f^i. \tag{5}$$

Assuming that Z is invertible, the desired solution is

$$J = Z^{-1} D f^i = P f^i, \tag{6}$$

where $P = Z^{-1}D$ specifies the coefficients of the surface current approximation excited by a weighted sum of incident plane waves. For this reason, P is referred to as the plane wave response matrix (P-matrix).

Figure 2 illustrates the plane wave response matrix for TM_z scattering from the target shown in Figure 1 when $\alpha = 20\lambda$ and $\beta = 1.5\pi$. Each column of this matrix provides an approximation of the electric current excited on the surface of the target for incident plane waves originating from $\phi = 0$ (the leftmost column) to $\phi =$
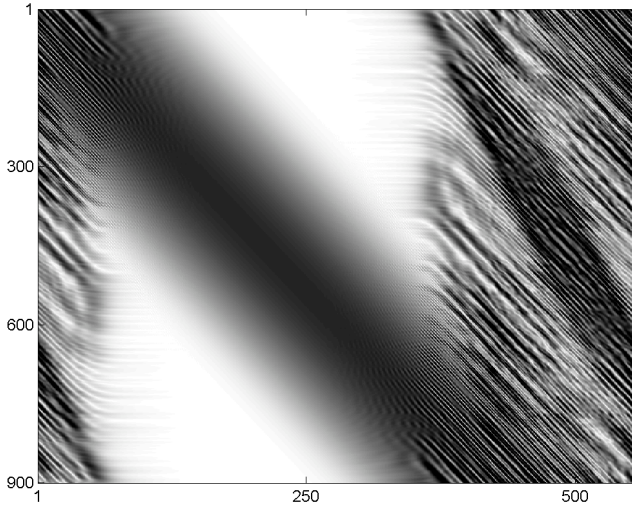
Figure 2. Absolute value of elements of plane wave response matrix for the target illustrated in Figure 1 when $a = 20\lambda$ and $\beta = 1.5\pi$. $N = 900$ uniformly spaced samples were used to discretize the target. $N_\phi = 558$ angles were used to sample the incident plane wave spectrum. The gray colorscale is mapped to the interval $[0, 15]$, with white indicating approximately zero amplitude, and black indicating an amplitude of 15 or more.

$1.5\pi(1 - 1/N_\phi)$ (the rightmost column). The first row of the P-matrix provides an approximation of the current excited on the first segment of the target (located at $\phi = 0$ in Figure 1) due to each of the discretely sampled incident plane waves. The last row of the P-matrix provides similar information for the segment of the scatterer located at $\phi = \beta$ in Figure 1. The approximately banded nature of P in Figure 2 is due to the quasi-specular scattering observed for plane waves incident onto smooth portions of the target.

4. ANGULAR AND SPATIAL GROUPS

Set-up for the beam transform method requires specification of groupings for both angular and spatial variables. To increase the efficiency of the resulting P-matrix compression algorithm, a multilevel organization is used to define the spatial groups. However, a single-level grouping is used to organize the angular data.

4.1. Angular Groups

Having restricted our attention to a single-level algorithm for two-dimensional scattering problems, specification of the far-field angular groups is straightforward. Let N_ϕ indicate the total number of uniformly spaced angular samples on the interval $[0, 2\pi)$ used to represent D and f^i in (4), and let M_ϕ denote the number of equally sized angular regions used to group these plane wave directions. The number of samples in each angular region is approximately $m_\phi = N_\phi/M_\phi$. The total number of angular samples is selected using the formula [3]

$$N_\phi = 2(2ka + 5\ln(2ka + \pi)) \tag{7}$$

where a is the cylinder radius in Figure 1. Equation (7) provides an estimate of the number of angular samples to characterize the electromagnetic response of a target to separated observers.

4.2. Spatial Groups

A binary tree is used to define spatial groups for the geometry indicated in Figure 1. This is accomplished by associating each point on the surface of the scatterer with an angle on the interval $[0, \alpha]$ and forming a binary tree for the angles on this interval.

The total number of points on the scatterer is N. The number of levels in the multilevel binary tree is L. The levels are indexed by l, $l = 1, \cdots, L$. The level $l = 1$ is the root level of the tree. The root level consists of a single group containing all spatial samples. The number of groups at the lth level of the tree is $M(l) = 2^{l-1}$, and the number of spatial samples in each group is approximately $m(l) = N/M(l)$. The index $i(l)$ is used to enumerate the groups at each level, $i(l) = 1, \cdots, 2^{l-1}$. Finally, the two level-l groups contained by a given group at level-$(l-1)$ are referred to as the level-l children of that level-$(l-1)$ parent. Groups at level-L have no children, and the root group has no parent. The total number of levels, L, is chosen so that the level-L groups have a maximum dimension of approximately one wavelength.

Although the binary tree just described is adequate for the set of problems indicated in Figure 1, a more general tree will be necessary for more complex targets. The multilevel spatial decomposition trees used with the multilevel fast multipole algorithm (MLFMA) [2] might provide an adequate representation for general geometries.

5. COMPRESSING THE P-MATRIX

The beam transform method for the P-matrix consists of defining beams of weighted plane waves originating from a given angular region which excite nonzero currents in only one of the spatial groups defined above. The desired beams are determined as a sequence of transformations. For a given tolerance ε, the first transform reduces the number of degrees of freedom (DoF) associated with a given angular region by retaining only those plane wave modes which contribute significantly to currents on the surface of the target. The second transform of the algorithm combines this reduced set of plane wave modes to form beams which excite nonzero currents on progressively larger sections of the scatterer surface. The basic computational tool used to form these beams is motivated by an algorithm developed by Canning [4]. Reference [4] provides an SVD-based method for determining beams associated with a given spatial region which radiate significant energy only to a small subset of all possible angular directions. Here we use a similar SVD-based algorithm in a different manner, forming combinations of beams impinging from a given set of directions to excite currents over a limited section of a large target. We have also found it necessary to develop a multiply resolved implementation of the algorithm to facilitate the determination of beams which illuminate successively larger spatial groups.

In the following discussion of the BTM, the notation $P_{\forall j}$ will be used to indicate the rectangular block of the P-matrix which identifies the currents excited at all points on the surface of the scatterer due to plane waves incident from angular group j. The dimension of this block is $N \times m_{\phi}$. Similarly, notation of the form $P_{i(l)j}$ will be used to represent currents excited in spatial group i at level-l due to plane waves incident from angular group j.

5.1. DoF Compression

The first stage of the BTM consists of determining a minimal set of plane wave modes originating from a given angular region which contribute to currents excited on the surface of the target with a relative mean square amplitude which exceeds a given tolerance ε. This reduced basis is obtained by performing a singular value decomposition of $P_{\forall j}$ [5],

$$P_{\forall j} = \hat{u}_{\forall j} \hat{s}_{\forall j} \hat{v}_{\forall j}^{H}, \tag{8}$$

and retaining those columns of $\hat{v}_{\forall j}$ having relative singular values exceeding ε:

$$\hat{s}_{\forall j} > \varepsilon \max(\hat{s}_{\forall j}). \tag{9}$$

Let the resulting ε-approximation of $P_{\forall j}$ be represented

$$P_{\forall j} \approx u_{\forall j} s_{\forall j} v_{\forall j}^H, \tag{10}$$

and denote the number of modes retained by r_j:

$$r_j = \operatorname{rank}(v_{\forall j}). \tag{11}$$

5.2. Beam-based Compression

An additional, beam-based compression of the $P_{\forall j}$ is determined by rewriting (10) as

$$P_{\forall j} v_{\forall j} s_{\forall j}^{-1} \approx u_{\forall j} \tag{12}$$

where we have used the fact that $s_{\forall j}$ is invertible because any zero singular values in $P_{\forall j}$ have been removed in passing from (8) to (10). The remaining matrix on the right side of (12) consists of the left singular vectors of the original matrix, $P_{\forall j}$. Since the range of P is the electric current on the target surface, the matrix $u_{\forall j}$ specifies how each column of $v_{\forall j}$ is distributed over the target surface. (The strength of each mode is specified by the diagonal elements of $s_{\forall j}$.) In the remainder of this section we define sparsifying transforms for $u_{\forall j}$. When combined with $v_{\forall j} s_{\forall j}^{-1}$ on the left side of (12), the resulting beam-based transforms will also sparsify $P_{\forall j}$.

The submatrices $u_{i(l)j}$ of $u_{\forall j}$ specify how the modes in $v_{\forall j}$ are distributed over that portion of the scatterer contained by the ith level-l spatial group, $i(l)$. Since we are interested in determining beams (i.e., combinations of the columns of $v_{\forall j}$) which excite currents only in specified spatial groups, it is useful to perform a final SVD of the blocks $u_{i(l)j}$:

$$u_{i(l)j} = U_{i(l)j} \Sigma_{i(l)j} V_{i(l)j}^H. \tag{13}$$

Substituting this in (12) provides

$$P_{i(l)j} v_{\forall j} s_{\forall j}^{-1} V_{i(l)j} \approx U_{i(l)j} \Sigma_{i(l)j}, \tag{14}$$

where $v_{\forall j} s_{\forall j}^{-1} V_{i(l)j}$ is the desired transform of $P_{i(l)j}$ into modes sorted by the degree to which they excite currents which are spatially localized

in group $i(l)$. To see this, recall that $u_{\forall j}$ is unitary. Thus, the singular values in $\Sigma_{i(l)j}$ are necessarily less than or equal to one. The singular values which are close to one correspond to modes $V_{i(l)j}$ which excite surface currents that are primarily localized in spatial group $i(l)$. (The actual distribution of this current within group $i(l)$ is specified by $U_{i(l)j}$.) Since the SVD indicated in (13) is assumed to sort modes in the order of decreasing singular values, $V_{i(l)j}$ provides a basis which is ordered according to the degree with which each mode localizes currents inside group $i(l)$. Let $\sigma_{i(l)j}$ denote the diagonal elements of $\Sigma_{i(l)j}$. Those modes in $V_{i(l)j}$ corresponding to singular values that satisfy

$$1 - \sigma_{i(l)j} < \varepsilon^2 \tag{15}$$

are considered to be spatially localized to order ε. (A tolerance of ε^2 is used because the final beam transform will have a condition number of approximately $1/\varepsilon$.)

Let $V_{(l)j}$ denote the collection of the $V_{i(l)j}$ obtained by performing the decomposition (13) for all level-l spatial groups which satisfy (15):

$$V_{(l)j} = \bigcup_{i(l)=1}^{M(l)} V_{i(l)j} \Big|_{\sigma_{i(l)j} > 1 - \varepsilon^2}. \tag{16}$$

Unfortunately, the rank of $V_{(l)j}$ is generally less than r_j. This occurs because, for a given problem, the number of spatially localized beams originating from a given angular region will depend on the tolerance ε, the size of the angular region, and the size of the spatial regions to which each beam is localized. For a single beam, maximum compression of $P_{\forall j}$ is obtained by using the finest possible spatial localization. However, using small spatial regions to define the $u_{i(l)j}$ in (13) reduces the total number of modes satisfying (15).

5.2.1. Multiresolution BTM

To accommodate these competing constraints, multiple spatial resolutions are used to determine the desired beam transform. The desired beam transform modes are determined by looping through the levels of the spatial tree of Figure 3, beginning at the finest level and ending at the root level. The first time through this loop (level-L), the basis $V_{(L)j}$ is determined as indicated in (16). This result is then used to initialize the basis V_j which is used to accumulate the beam transform modes as we proceed up the spatial tree. At each level, the V_j basis is used to define an updated version of $u_{\forall j}$:

$$u_{\forall j} \Leftarrow u_{\forall j} - u_{\forall j} V_j V_j^H. \tag{17}$$

level l=2 group

Scatterer

level l=1 group

level l=L groups

level l=L-1 groups
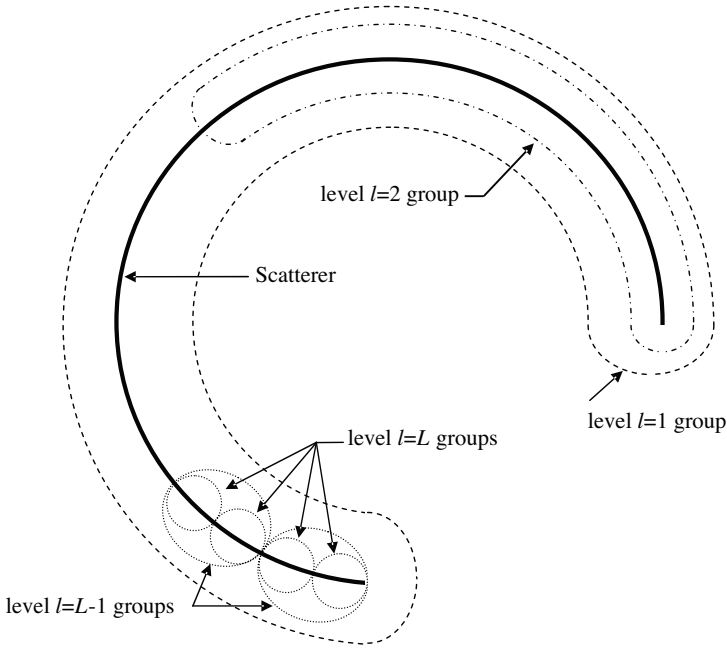
Figure 3. Illustration of multilevel binary tree used to define spatial groups on surface of scatterer.

This updated matrix is then analyzed at the next (coarser) level using the procedure indicated by Equations (12) to (16). The resulting $V_{(L-1)j}$ are appended to V_j, the matrix $u_{\forall j}$ is updated according to (17), and the procedure continues to the next level of the tree. For a given angular group j, this procedure is continued until the rank of V_j is equal to r_j. Because the root level contains all points on the surface of the scatterer, we are guaranteed to always find the required number of modes. To obtain good compression, we would like most of the elements in V_j to come from the finer levels of the spatial tree. In practice, this will largely be a function of the physical properties of the scattering problem.

Having determined V_j, the final beam transform associated with a given angular region is computed as

$$\Lambda_j = v_{\forall j} s_{\forall j}^{-1} V_j. \tag{18}$$

The required inverse transform is

$$\Lambda_j^{-1} = V_j^H s_{\forall j} v_{\forall j}^H. \tag{19}$$

---

for j=1: M_ϕ

    ```
compute truncated svd of (10)
```
    for l =L:-1:1

        ```
Compute
```
$V_{(l)j}$ ```using (12) to (16)```

        ```
Append to
```
V_j : $V_j = V_j \cup V_{(l)j}$

        ```
Update
```
$u_{vj} \Leftarrow u_{vj} - u_{vj}V_jV_j^\dagger$

    end

    ```
Compute
```
Λ_j ```and``` Λ_j^{-1} ```via (18) and (19)```

end

```
Accumulate
```
Λ_j ```and``` Λ_j^{-1} ```as diagonal blocks of beam transform matrices``` Λ ```and``` Λ^{-1}

Figure 4. BTM procedure for determining the diagonal blocks of the beam transform matrices Λ and Λ^{-1}.

Block diagonal beam transform matrices Λ and Λ^{-1} are used to accumulate the transforms obtained from each angular region. The numerical examples included below demonstrate that $P\Lambda$ is often sparse, and that $(P\Lambda)\Lambda^{-1}$ provides an order-ε implementation of P.

Figure 4 summarizes the multiresolution BTM procedure for determining the respective block diagonal transform and inverse transform matrices Λ and Λ^{-1} obtained by accumulating the diagonal blocks Λ_j and Λ_j^{-1} for all angular regions.

5.3. Beam Transform of P-matrix

Let B denote the beam transform of P,

$$B = P\Lambda. \tag{20}$$

In the following we refer to B as the beam footprint matrix. A sparse, order-ε representation of P is obtained by retaining in each column of B only those rows which are in the spatial group $i(l)$ towards which a given beam in Λ is directed. These elements can be computed directly from (20) once Λ is known. A somewhat more efficient alternative is to compute the nonzero elements of B using the right side of (14) for each element of $\hat{V}_{i(l)j}$ satisfying (15). In the following numerical examples we use the latter method to determine the nonzero elements of B.

6. NUMERICAL EXAMPLES

The properties of the BTM for the P-matrix are illustrated using several examples derived from the target configuration of Figure 1. We also consider an application of the P-matrix to a problem involving point source excitations.

6.1. Properties of the BTM

Figure 5 displays the nonzero elements of B for scattering from the geometry indicated in Figure 1 when $\alpha = 20\lambda$, $\beta = 2\pi$ and an input tolerance of $\varepsilon = 0.01$ is used. $N = 1200$ pulse basis functions are used to expand the surface current, representing a sampling interval of 0.105λ along the surface of the target. The multilevel spatial tree has $L = 6$ levels, with a total of 32 groups at the finest level of the tree. A total of $N_\phi = 558$ angular samples are used, and they are grouped into $M_\phi = 4$ angular regions. The actual RMS error obtained after compressing the P-matrix is 0.0044. The maximum RMS error in
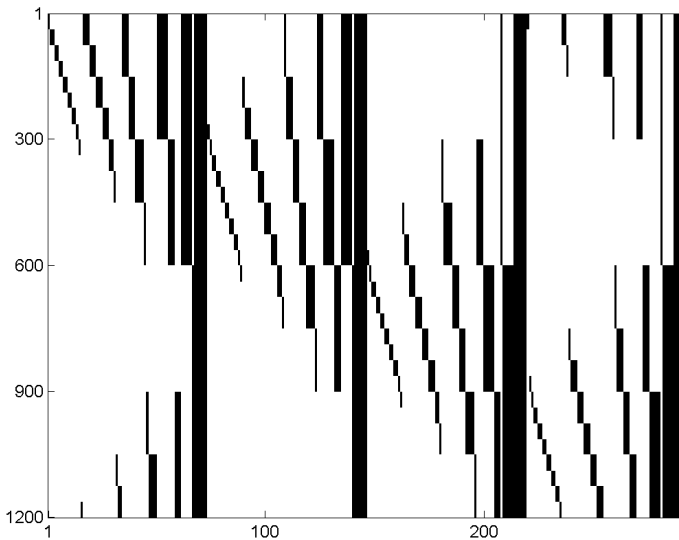
Figure 5. Beam footprint matrix, B, for plane wave scattering from the PEC shell of Figure 1 when $a = 20\lambda$ and $\beta = 2\pi$. $N = 1200$ points are used to discretize the target, and $N_\phi = 558$ angular samples are used in forming P. The nonzero elements of the B matrix which are retained for a requested tolerance of $\varepsilon = 0.01$ are shown in black. The zero elements of B are white.

representing a given column of the P-matrix is 0.0055, indicating the maximum RMS error encountered in using the compressed P-matrix to calculate the current excited by a plane wave incident from any direction.

For this example, the inverse transform matrix Λ^{-1}(not shown) has size 292×558. The nonzero elements of Λ^{-1} occur in four blocks along the diagonal of the matrix. Two of the four diagonal blocks have dimension 73×140, and two others have dimension 73×139. A total of 1.18×10^5 complex numbers are required to represent both B and Λ^{-1}. The total number of nonzero elements required to directly store Z^{-1} is 1.44×10^6, and the number required to store P is 6.70×10^5.

Figure 6 shows the transformed P-matrix for the case illustrated in Figure 2 ($a = 20\lambda$, $\beta = 1.5\pi$). An input tolerance of $\varepsilon = 0.01$ was used. The actual RMS error after the BTM compression is 0.0049. The maximum error in representing any column of the P-matrix is 0.0060. The total number of nonzero elements used to store B and Λ^{-1} is
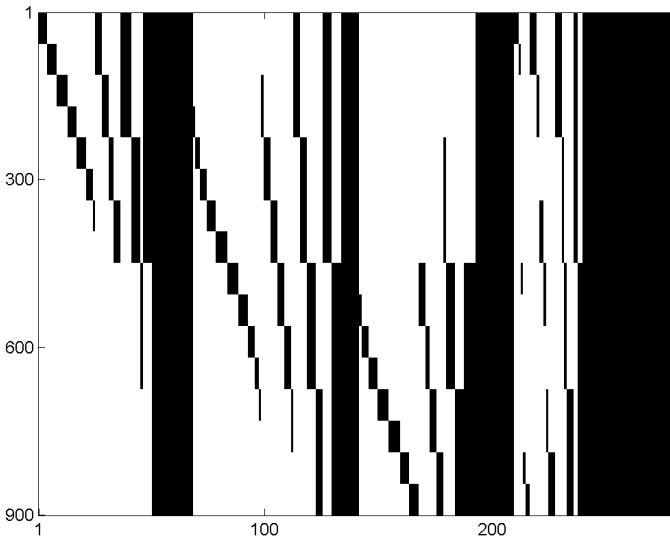
Figure 6. Beam footprint matrix, B, for plane wave scattering from the PEC shell of Figure 1 when $a = 20\lambda$ and $\beta = 1.5\pi$. $N = 900$ points are used to discretize the target. $N_\phi = 558$ angular samples are used, and $M_\phi = 4$ angular groups are used to define the beam transform matrix Λ. The nonzero elements of the B matrix which are retained for a requested tolerance of $\varepsilon = 0.01$ are shown in black. The zero elements of B are white.

1.43×10^5, which is larger than the number required for the example considered in Figure 5. The primary reason for this increase is that in the present case ($\beta = 1.5\pi$) the scatterer is an open cavity, and fewer beams can be formed which excite currents at the finer levels of the spatial tree. In particular, we observe from Figure 6 that, of the four angular groups used, the angular region which has the largest number of modes which are nonzero over the entire surface of the target is the last (fourth) group. This group corresponds to sums of plane waves which are incident from the angular sector $1.5\pi < \phi < 2\pi$, which corresponds to the open end of the cavity (cf. Figure 1).
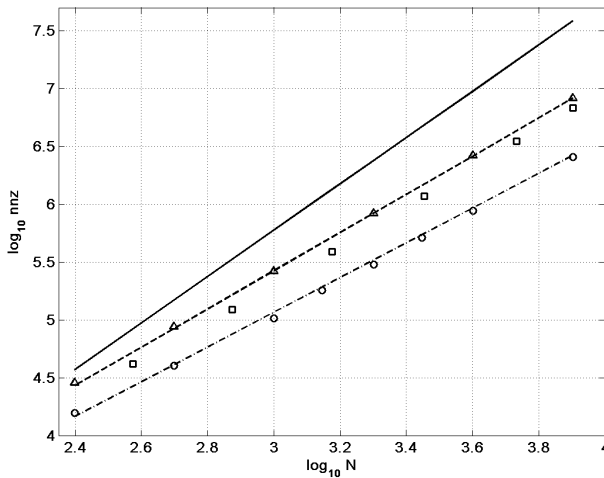
Figure 7. Complexity scaling of BTM representation of P-matrix for geometries indicated in Figure 1 when $\beta = \pi$ (triangles), $\beta = 1.5\pi$ (squares) and $\beta = 2\pi$ (circles). The solid line is the equation $nnz = 0.6N^2$, the dashed line is $nnz = 3N^{1.65}$, and the dashed-dotted line is $nnz = 3.7N^{1.5}$.

The complexity scaling of the BTM is illustrated in Figure 7 for three different target geometries. In all cases, the surface of the target is discretized using 8 points per wavelength and a tolerance of $\varepsilon = 0.01$ is used (the actual RMS error in the BTM representation of the P-matrix varies between 0.004 and 0.00993). For the case $\beta = 2\pi$ the observed complexity scaling is $O(N^{1.5})$. A faster scaling of approximately $O(N^{1.65})$ is observed when $\beta = \pi$ and $\beta = 1.5\pi$.

It is expected that additional compression may be possible for the cases $\beta = \pi$ and $\beta = 1.5\pi$ considered in Figure 7. The BTM discussed

above has been designed to identify spatially contiguous beams originating from a given angular region. While this is effective for convex targets, configurations that exhibit strong multiple scattering may benefit from a modified version of the BTM designed to search for beams that excite small but disconnected spatial footprints.

Another extension of the BTM that is expected to improve the performance of the algorithm for all β is a multilevel organization of the angular groups. For example, Figure 8 illustrates the transformed P-matrix for the same problem considered in Figure 6 when a single angular region ($M_\phi = 1$) is used to form the beam transform Λ. B is evidently more sparse in this case than the result obtained in Figure 6 using $M_\phi = 4$ angular groups. The price paid to obtain the sparse form of B in Figure 8 is a full inverse beam transform matrix Λ^{-1}. It may be possible to lower the cost to implement Λ^{-1} by using either a multilevel organization of the angular information or bandlimited angular functions [6].
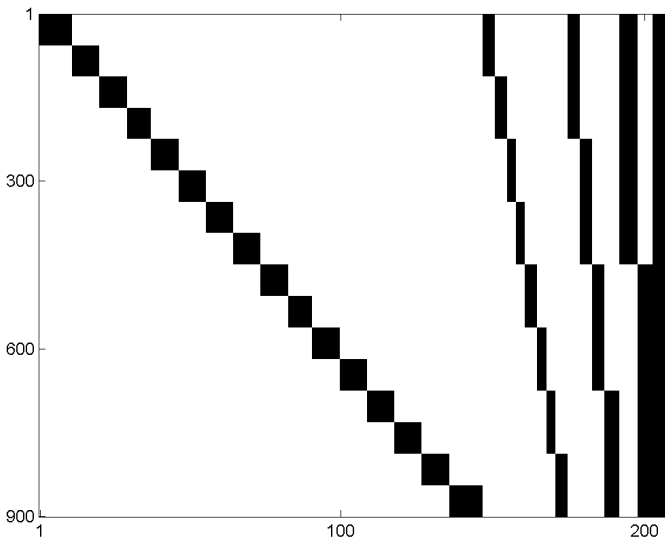
Figure 8. Same as Figure 6, but with $M_\phi = 1$.

6.2. Finite Sources

A drawback to the P-matrix representation of the scattering problem is the assumption that the problem excitation can be represented as a sum of propagating plane waves (cf. (5)). For example, this implies that, as presented here, the P-matrix associated with Figure 5 cannot

be directly used to accurately determine the currents excited by a point source located very close to the target surface. To quantify this property, we again consider the scattering configuration obtained when $\beta = 1.5\pi$.

We would like to determine the solution to this scattering problem for an impressed point source located on the x-axis. Because the P-matrix is defined in terms of plane wave excitations, we first seek solutions to the problem

$$M^i = Df^i, \tag{21}$$

where M^i is the field radiated by the point source and sampled on the target surface, and f^i is the unknown plane wave excitation. For a given M^i, we determine a least-squares solution to (21) using the pseudo-inverse of D [5],

$$f^i = D^\dagger M^i. \tag{22}$$

The existence of numerically accurate solutions to (21) will depend on the properties of M^i. In cases for which (22) is an accurate solution of (21) we have

$$Z^{-1}M^i \approx PD^\dagger M^i. \tag{23}$$

Figure 9 shows the RMS error obtained when the compressed P-matrix indicated by Figure 6 is used to estimate the electric current excited on the target by a point source located at $y = 0$ as a function of position x on the interval $-40\lambda < x < 40\lambda$. In all cases, the reference solution is obtained by directly computing $Z^{-1}J^i$. Referring to the figure, when the point source is located more than about two wavelengths outside the PEC shell, the error is approximately 0.005. The larger error observed when the point source is located near $x = \pm20$ can be traced back to our inability to find accurate solutions to (22). We also observe that accurate solutions (relative to the reference solution) are obtained when the point source is more than a few wavelengths "inside" the open PEC shell. Although we only show results for the case $\beta = 1.5\pi$, similarly accurate results have been obtained for all values of β, including the case $\beta = 2\pi$. The compressed P-matrix for the latter case is shown in Figure 5.

While these results indicate that the P-matrix representation may prove useful for problems excited by local sources, the scheme outlined above requires an implementation of the pseudo-inverse $D^\dagger$ in (22). This was accomplished in the preceding numerical examples by computing the singular value decomposition of D. To be numerically efficient, the scheme reported above will require a more efficient implementation of this operation.
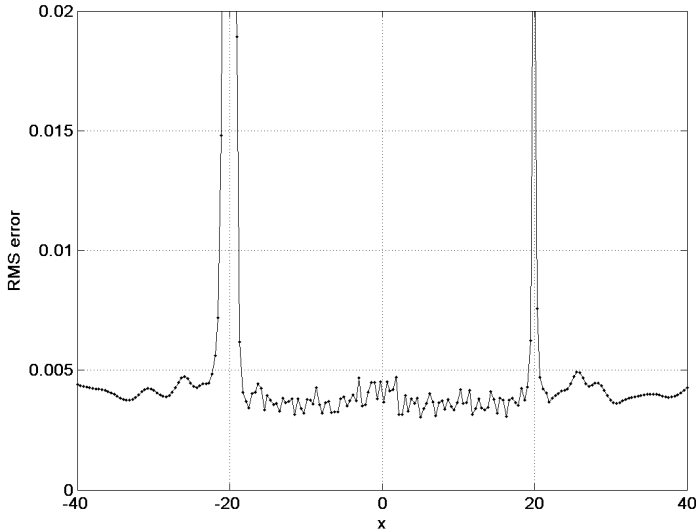
Figure 9. RMS error in surface current vector J as function of point source location on the x-axis..

7. SUMMARY AND DISCUSSION

The beam transform method (BTM) provides a compressed representation of the plane wave response matrix for electrically large targets. The BTM is based on the physical principle that it is often possible to determine beams originating from a given angular region which excite spatially localized currents on the surface of a target. Numerical examples indicate that the complexity of the resulting BTM representation of the P-matrix increases at rates which vary between $O(N^{1.5})$ and $O(N^2)$. The lowest complexity, $O(N^{1.5})$, was observed for the closed PEC cylinder. In this case the scattering is dominated by single-bounce effects. The complexity scaling was somewhat faster for geometries which excite strong multi-bounce interactions. We anticipate that a more efficient version of the BTM can be obtained in a number of ways. For example, it may be beneficial to use a multilevel grouping of the angular regions instead of the single-level grouping used here. Other methods for improving the performance of the method are discussed elsewhere [6].

The numerical examples provided above indicate that the BTM representation of the P-matrix can be used to determine the currents excited on the surface of a target by a point source. This capacity of the BTM representation depended on our ability to determine an accurate

equivalent plane wave representation of the incident fields excited by the point source. For the open PEC cylinders considered here, this was observed to be possible even when the point source excitation was located on the interior of a large cavity. However, it remains to be determined if the required pseudo-inverse operation indicated in (22) can be implemented efficiently.

The BTM discussed herein is a single-bounce (SB) algorithm because the beam transforms used to compress the P-matrix are determined by seeking solutions which are localized to a single group, $i(l)$, at level-l. Consider the more general case of a spectral mode which is localized within two spatially disconnected level-l groups, $i(l)$ and $j(l)$. We refer to these as two-bounce ($2B$) modes. The SB BTM cannot incorporate a $2B$ mode until the algorithm reaches the coarse level having a single group which contains the disconnected level-l groups. This is one reason that the efficiency of the SB BTM decreases when applied to targets which exhibit strong multiple scattering. A multibounce version of the algorithm reported here will be considered elsewhere.

Finally, an important limitation of the method discussed here is that the P-matrix was obtained by first inverting the impedance matrix, Z^{-1}, and then multiplying by the plane wave transform matrix D_α. While such an approach may be feasible for a restricted class of problems, the applicability of the BTM would be significantly extended if these set-up costs were reduced. Reference [7] outlines a procedure for more efficiently determining localizing spectral modes.

REFERENCES

1. Peterson, A. F., S. L. Ray, and R. Mittra, *Computational Methods for Electromagnetics,* IEEE Press, New York, 1998.
2. Chew, W. C., J. M. Jin, E. Michielssen, and J. Song, "Fast and efficient algorithms in computational electromagnetics," Artech House, Boston, 2001.
3. Coifman, R., V. Rokhlin, and S. Wandzura, "The fast multipole method: a pedestrian prescription," *IEEE Antennas and Propagation Magazine,* Vol. 35, 7–12, 1993.
4. Canning, F. X., "Compression of interaction data using directional sources and testers," Non Provisional US Patent Application, USA, 2003.
5. Golub, G. H. and C. F. Van Loan, *Matrix Computations,* Third edition, Johns Hopkins, University Press, 1996.
6. Adams, R. J., G. Wang, F. X. Canning, and B. A. Davis, "Single-

bounce bandlimited beam transform method," *Radio Science,* submitted for publication.

Robert J. Adams received his B.S. degree from Michigan Technological University in 1993. He received M.S. and Ph.D. degrees in electrical engineering from Virginia Tech in 1995 and 1998. From 1999 through 2000 he was a Research Assistant Professor at Virginia Tech. He is currently an Assistant Professor of Electrical & Computer Engineering at the University of Kentucky. His research interests are in applied and computational electromagnetics.

Francis X. Canning received the A.B. degree from Dartmouth College in March, 1971, completing the mathematics and physics majors. He received the M.S. (1976) and Ph.D. (1982) degrees in physics from the University of Massachusetts at Amherst. He is currently the sole proprietor of Simply Sparse Technologies, Inc., in Morgantown, WV.

Faisal A. Mev received the Bachelor of Engineering degree in Electronics & Instrumentation Engineering from Devi Ahilya University, Indore, India in 2002. He is currently working on his MS in Electrical Engineering at the University of Kentucky. His research interests are in electromagnetics.

Bradley A. Davis received his Ph.D. in 2000 from the Virginia Polytechnic Institute and State University, Blacksburg, VA. From 1986–1988 and again from 1996–2000, he was a research assistant in the ElectroMagnetics Interactions Laboratory (EMIL). In the intervening period, he worked for Westinghouse Defense Electronics in Baltimore, MD in antenna design and development. After leaving Westinghouse, he joined the System Engineering group at Central Maine Power where he performed electromagnetic assessment of facilities and system transient studies. After receiving the Ph.D., he was a research faculty member at Virginia Tech. Currently, he is the Director of Engineering at NanoSonic, Inc. where he continues to work in computational electromagnetics and with unique nano-structured materials with customized electromagnetic properties.